Mineralia Slovaca, Web ISSN 1338-3523, ISSN 0369-2086, https://doi.org/10.56623/ms.2026.58.1.2
58, 1 (2026), 37 – 50,

Picritic rocks (meimechites) from Poniky: mineralogy and petrology (Western Carpathians)

†JÁN SPIŠIAK[1], JURAJ BUTEK[1,*], VIERA ŠIMONOVÁ[1], RICHARD KOPÁČIK[1], ANGELIKA OBERTOVÁ[1] and SERGIY KURYLO[2]

[1] Department of Geography and Geology, Faculty of Natural Sciences, Matej Bel University, Tajovského 40, 974 01 Banská Bystrica, Slovak Republic,

[2] Earth Science Institute, Slovak Academy of Sciences, Ďumbierska 1, 974 11, Banská Bystrica, Slovak Republic

* Corresponding author, juraj.butek@umb.sk

Abstract: New data on picritic rocks from the Poniky area are presented in this contribution. In addition to the major mafic minerals (clinopyroxene, kaersutite, phlogopite), spinels, Sr-rich apatite (up to 6.4 wt% SrO), and sodalite are also described. Sodalite is documented for the first time in the Central Western Carpathians, and together with the mineralogical and whole-rock compositions, it confirms the alkaline character of these rocks. Petrological data, including REE, show that they are equivalent to the Cretaceous volcanic rocks occurring in the Fatric Unit as well as to picritic rocks of the teschenite-picrite association occurring in the External Western Carpathians. The high MgO content (>18 wt%) allows these rocks to be classified as meimechites.

Key words: picrite, mineralogy, whole-rock geochemistry, Cretaceous, Western Carpathians

Introduction

Picrite is a hypoabyssal rock, often porphyritic, with a high content of mafic minerals and an elevated MgO content compared to basalts (>12 wt%; Le Bas, 2000). Its occurrences are rare in the Western Carpathians. Picrites occur in the External Western Carpathians as part of the Cretaceous teschenite-picrite association within the Silesian Unit (Brunarska & Anczkiewicz, 2019; Buriánek et al., 2013; Hovorka, 1976; Hovorka & Spišiak, 1988; Kudělásková, 1987; Mahmood, 1973; Šmíd, 1962; Szopa et al., 2014). In the Central Western Carpathians, only limited occurrences of picrite were reported from boreholes in Mesozoic sedimentary sequences near Banská Bystrica (Hovorka & Slavkay, 1966; Hovorka & Spišiak, 1988; Slavkay, 1979). These picritic rocks are Cretaceous in age and are genetically associated with alkaline volcanism. A solitary occurrence of a metamorphosed picrite was also documented in the Gelnica Group of the Gemeric Unit (Ivan, 1991).

A substantial amount of information on the picrite occurrence near Banská Bystrica was published by Spišiak & Hovorka (2000) and in the monograph Mesozoic Volcanism of the Western Carpathians (in Slovak; Hovorka & Spišiak, 1988). Despite this, we present new and interesting mineralogical and petrological data on an older picritic sample from a borehole near Poniky.

Geological setting

Picritic rocks from the vicinity of Banská Bystrica were documented in both boreholes Po-1 and St-2 in the Poniky area (Fig. 1A; Spišiak & Hovorka, 2000; Slavkay et al., 1968). The analysed sample came from the Po-1 borehole, located approximately 250 m west of the northern edge of Poniky (48.715751 °N, 19.287881 °E; Fig. 1B). The rocks occur at a depth of 460 m. The host rocks are significantly brecciated Middle Triassic dolomites. These dolomites were originally affiliated with the Hronic Unit (Hovorka & Slavkay, 1966).

The geological structure of the broader Poniky area is characterized by the tectonic superposition of three units: the Fatric Unit, the Hronic Unit, and the Silicic Unit. The Fatric Unit comprises Middle Triassic to Cretaceous deposits. Shallow-water organodetritic carbonates are typical of the Triassic. The Jurassic-Lower Cretaceous succession continues with shallow-water crinoidal and nodular limestones, which are gradually replaced by deeper-water clayey limestones, mudstones, and shales (Slavkay, 1971). The Hronic Unit is structurally higher. The succession begins with Middle Triassic dark-grey limestones. These are overlain by strongly weathered dolomites, which represent the host rock of the aforementioned biotitic picrites. According to Hovorka and Slavkay (1966), these represent submarine lava flows emplaced into the Triassic sedimentary environment. The succession continues with Upper Triassic carbonates. The uppermost unit is the Silicic Unit. Its lower part comprises Lower Triassic variegated arkosic sandstones, shales, mudstones, and clayey limestones with abundant Campilian fauna (Slavkay, 1971). These complexes also include extensive Permian volcanic rocks (Ondrejka et al., 2022). At the base, violet-brown paleoandesites occur, separated from alkaline rhyolites and their pyroclastics by clayey limestones (Slavkay, 1971). Shallow-water carbonate complexes rich in organic debris are again typical of the Middle and Upper Triassic age.

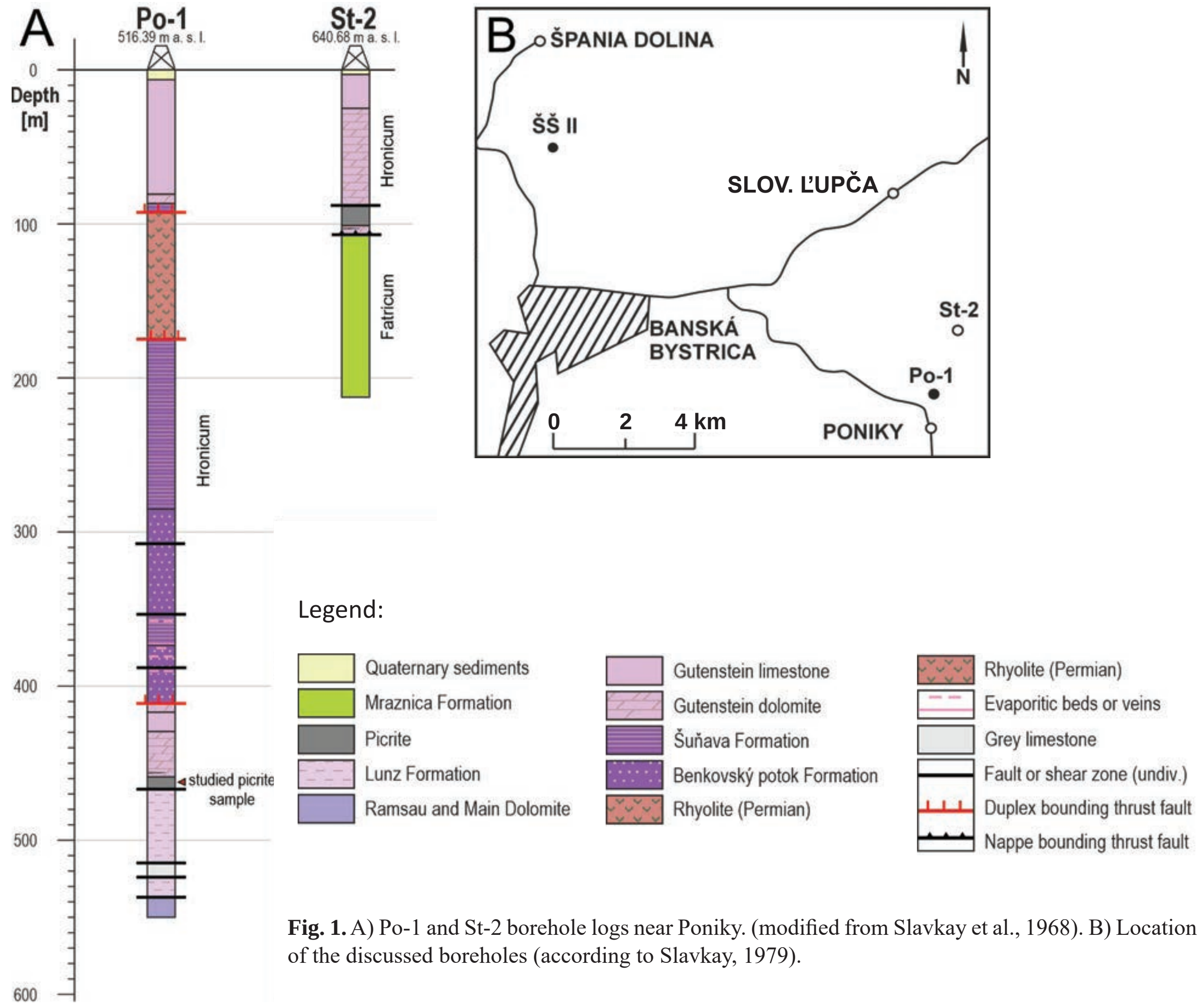

Fig. 1. A) Po-1 and St-2 borehole logs near Poniky. (modified from Slavkay et al., 1968). B) Location of the discussed boreholes (according to Slavkay, 1979).

Methods

Silicate minerals and apatite were analysed using a JEOL JXA-8530F electron microprobe at the Earth Sciences Institute of the Slovak Academy of Sciences in Banská Bystrica under the following conditions: accelerating voltage 15 kV, probe current 20 nA, beam diameter 3–8 µm, counting time 10 s on the peak and 5 s on the background. Raw counts were converted to oxide wt% using a ZAF matrix correction. The EPMA was calibrated using natural and synthetic minerals. Whole-rock analysis was performed at the Bureau Veritas Analytical Laboratories (Vancouver, Canada). Total abundances of major-element oxides were determined by inductively coupled plasma emission spectrometry (ICP-ES) following lithium metaborate-tetraborate fusion and dilute nitric acid treatment.

Results

Petrography and mineralogy

Analysed picritic rocks exhibit a porphyritic texture with olivine and clinopyroxene phenocrysts. Olivine (approximately 35 %) predominates over pyroxene. Other major minerals include biotite, amphibole, spinel, and sodalite.

Olivine is extensively serpentinised, forming typical mesh textures. Because only textural relics are preserved, olivine analyses are unavailable.

Two types of clinopyroxene occur in the rocks. The first type (Cpx I) occurs as small, inclusion-free phenocrysts (Fig. 2A). In contrast, the second type (Cpx II) forms large phenocrysts (2 – 5 mm) that poikilitically enclose other minerals, mainly sodalite, carbonate, chlorite and pyrite (Fig. 2B). Clinopyroxenes are weakly zoned; rims have slightly higher TiO_2 content. The chemical compositions of both clinopyroxenes are similar (Tab. 1). According to the IMA classification (Morimoto, 1988; Fig. 3), they are classified as diopside.

Amphibole coexists with clinopyroxene (Cpx I, Fig. 2A). It has elevated TiO_2 (up to 4.5 wt%) and Na_2O (up to 3.4 wt%; Tab. 2). According to the amphibole classification by Hawthorne et al. (2012), the analysed amphibole, with Ti reaching 0.5 apfu, falls at the boundary between pargasite and kaersutite. It is compositionally similar to amphiboles from Cretaceous alkaline rocks in the Fatric unit (Višňové, Krpeľany, Salatín, etc.) (Hovorka & Spišiak, 1988; Spišiak & Hovorka, 1997).

Biotite occurs as tabular phenocrysts together with clinopyroxene (Cpx I) and amphibole (Fig. 2A, 5B). It is dark brown to reddish brown, strongly pleochroic, and partially altered. It has high MgO (up to 16.69 wt%) and Na_2O (up to 1.5 wt%) contents, with an average TiO_2 content of 2.3 wt% that locally reaches up to 4 wt% (Tab. 3). Based on the mica classification by Tischendorf et al. (2007), it is classified as phlogopite (Fig. 4).

Sodalite occurs as discrete grains or as inclusions in diopside (Fig. 5). The composition of both types of sodalite is similar (Tab. 4) and matches that of sodalite in alkaline basic rocks (Deer et al., 2013). Sodalite is a common mineral in alkaline rocks and thus serves as an index mineral for the geochemical classification of the studied picritic rocks.

Spinel forms irregular grains that coexist with clinopyroxene and biotite (Fig. 6). It has high Al_2O_3 and elevated MgO, Cr_2O_3, and FeO contents (Tab. 5). Spinel is strongly altered at the rims; marginal parts show higher MnO, SiO_2, and TiO_2 contents and lower Cr_2O_3, MgO, and Al_2O_3 contents. According to the nomenclature and classification by Bosi et al. (2019), with Mg as the dominant bivalent cation and Al as the trivalent cation, it is classified as spinel *sensu stricto*. The chemical composition reflects that of a peridotitic spinel, consistent with the genetic classification of Deer et al. (2013) and with spinels from MORB and peridotites, as classified by Kamenetsky et al. (2001). Spinels from other occurrences of Cretaceous alkaline rocks in the Western Carpathians show a similar chemical composition (Mikuš et al., 2006).

Apatite forms subhedral to euhedral grains (Fig. 7). Given its chemical composition, apatite plots at the boundary between hydroxyapatite and fluorapatite (Fig. 8) and shows elevated LREE contents (Tab. 6). Apatite also exhibits distinct chemical zonation, primarily driven by variations in SrO content. SrO-rich rims reach up to 6 wt% SrO, whereas the cores are relatively SrO-poor (around 0.5 wt%). The increase in SrO is compensated by a corresponding decrease in CaO. Apatite from Cretaceous basic volcanics in the Western Carpathians is also characterized by elevated REE contents (Kynický et al., 2009; Szopa et al., 2014).

Pyrite is abundant in the form of veins (Fig. 6). Chlorite, serpentine-group minerals and calcite are common minor mineral phases.

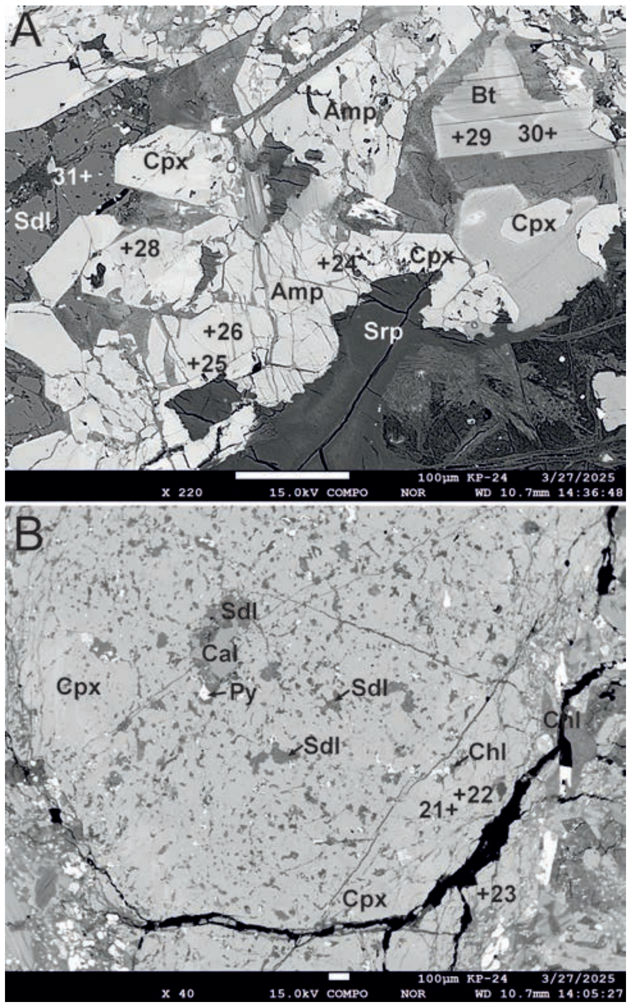

Fig. 2. Backscattered electron images of clinopyroxenes. A) Cpx phenocrysts without inclusions (Cpx I) coexisting with amphibole, phlogopite, and sodalite; B) a poikilitic clinopyroxene phenocryst (Cpx II) with inclusions of sodalite, pyrite, and calcite. Cpx – clinopyroxene, Amp – amphibole, Bt – biotite, Sdl – sodalite, Srp – serpentine, Chl – chlorite, Py – pyrite, Cal – calcite. Numbers in the figures correspond to the number of analyses in Tables 1, 2, and 3.

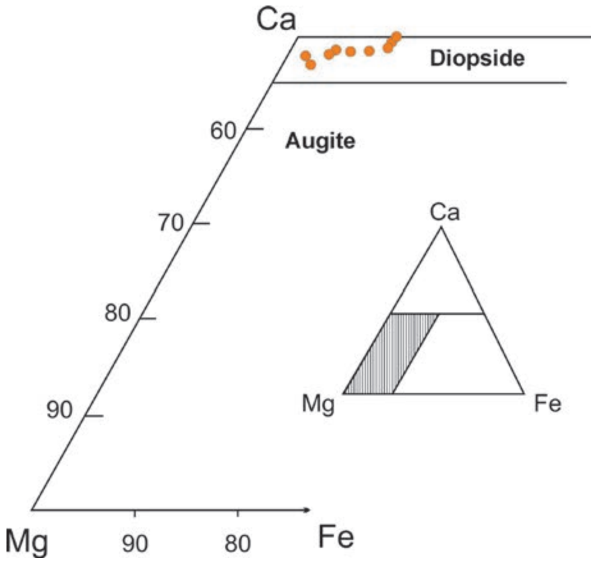

Fig. 3. Classification diagram of clinopyroxenes (after Morimoto, 1988).

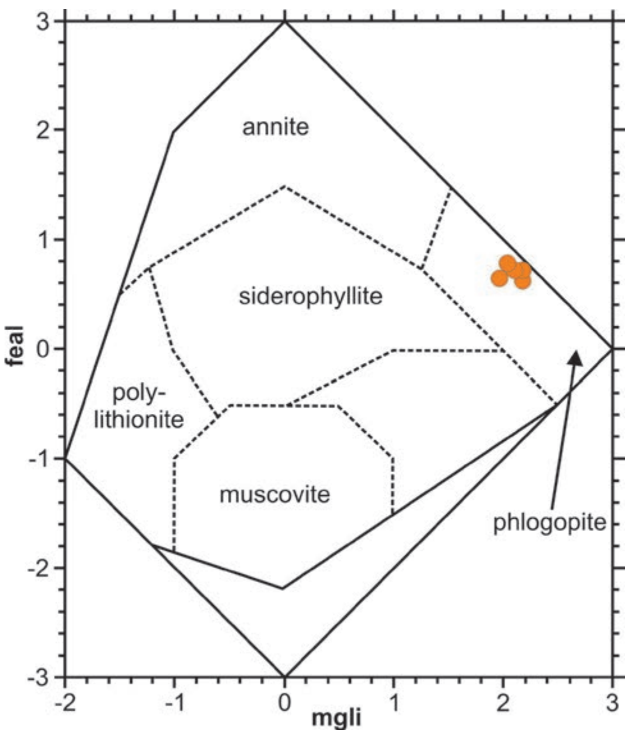

Fig. 4. Classification diagram of micas (after Tischendorf et al., 2007).

Whole rock geochemistry

The whole-rock chemical compositions of picritic rocks from the studied area are shown in Tab. 7. The whole-rock Mg# [molar Mg/(Mg + Fe)] ranges from 0.75 to 0.82. Based on the IUGS classification of high-MgO and low-SiO_2 rocks (Le Bas, 2000), the samples are classified as meimechites (Fig. 9). TiO_2 contents above 1 wt% and the absence of spinifex structures (Kerr & Arndt, 2001) exclude the name komatiite. This is the first description of meimechite in the Central Western Carpathians.

We use the ternary diagram TiO_2 vs MnO x 10 vs P_2O_5 x 10 (Mullen, 1983) for geotectonic classification (Fig. 10). The diagram shows that analyses of the studied rocks plot within the Ocean Island Alkaline Basalts field, consistent with their assumed geotectonic setting. Furthermore, the chondrite-normalized REE pattern shows significant enrichment in light REEs, a steeply descending curve, and no Eu anomaly (Fig. 11A). The chondrite-normalized spider diagram shows strong enrichment in incompatible elements and no visible Nb anomaly (Fig. 11B). It also displays positive Nd and Y anomalies.

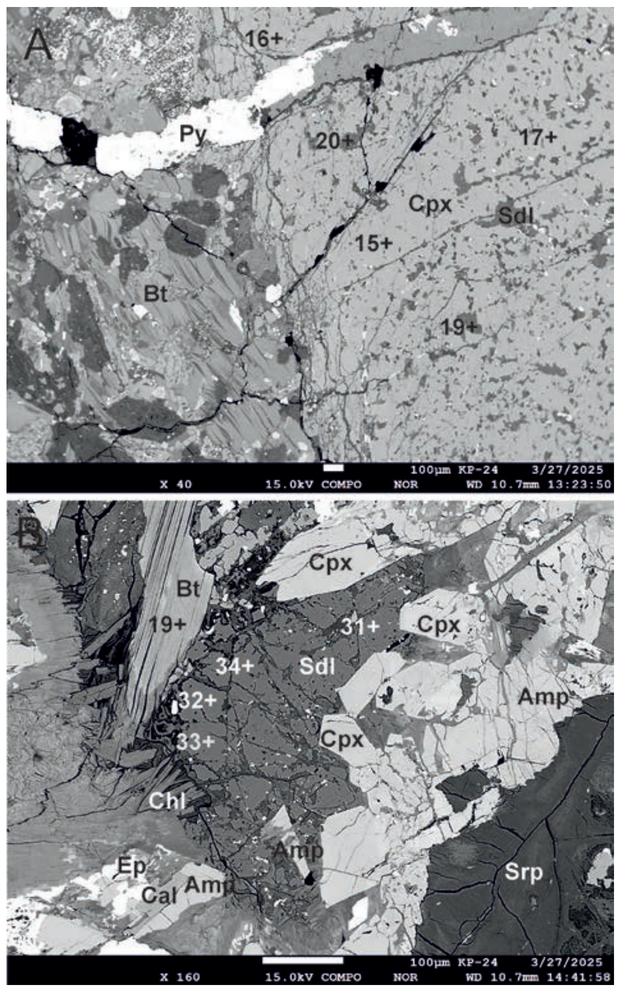

Fig. 5. Backscattered electron images of sodalite. A) Cpx phenocrysts with inclusions of sodalite, pyrite and calcite; B) a large single grain of sodalite. Cpx – clinopyroxene, Amp – amphibole, Bt – biotite, Sdl – sodalite, Srp – serpentine, Chl – chlorite, Py – pyrite, Cal – calcite, Ep – epidote. Numbers in the figures correspond to the number of analyses in Tables 1, 3 and 4.

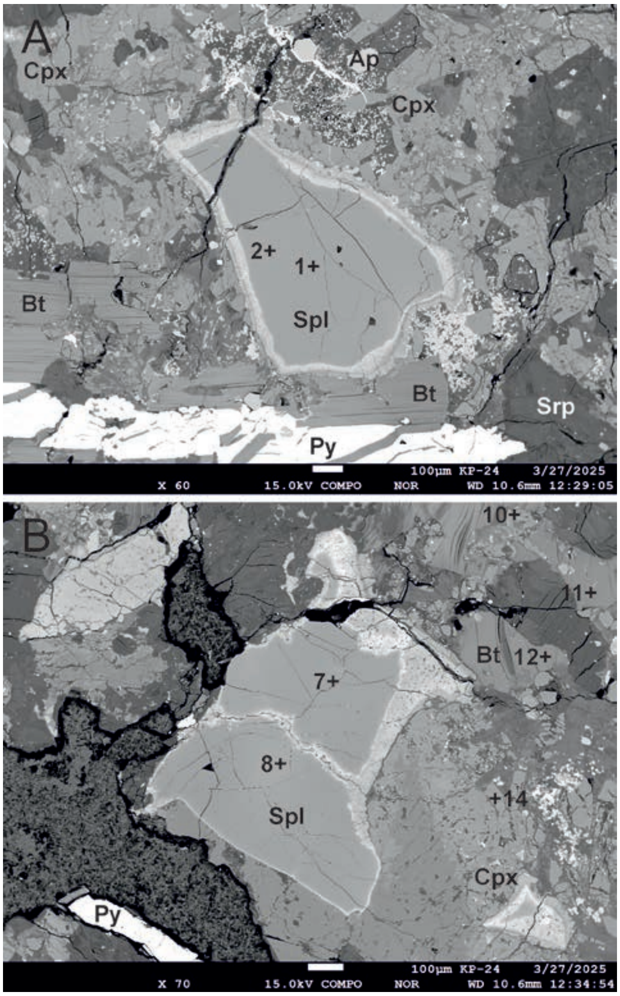

Fig. 6. Backscattered electron images of spinel. Cpx – clinopyroxene, Amp – amphibole. Numbers in the figures correspond to the number of analyses in Table 5.

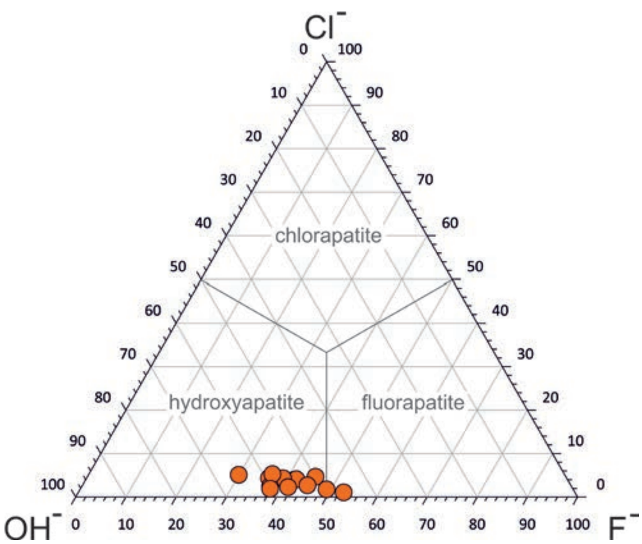

Fig. 8. Classification diagram of apatites from the studied picrites.

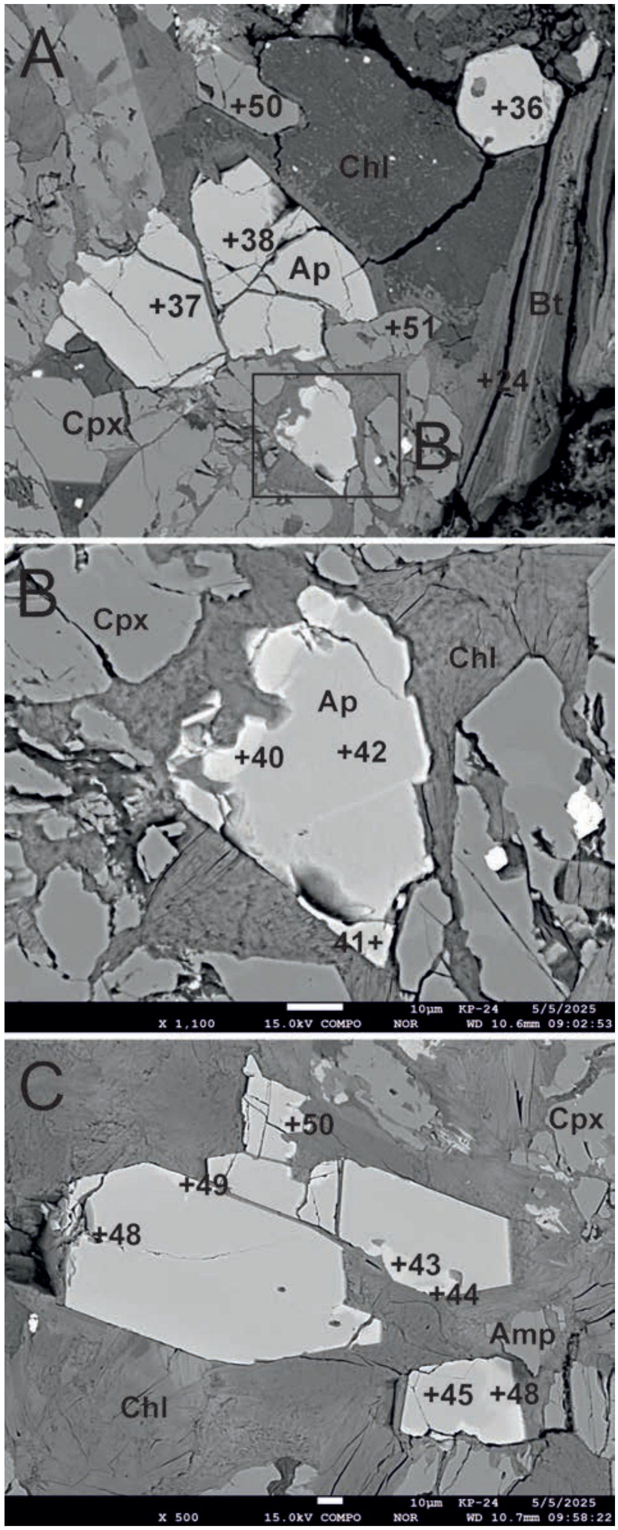

Fig. 7. Backscattered electron images of apatite. Spl – spinel, Cpx – clinopyroxene, Ap – apatite, Bt – biotite, Srp – serpentine, Py – pyrite. Numbers in the figure correspond to the number of analyses in Table 6.

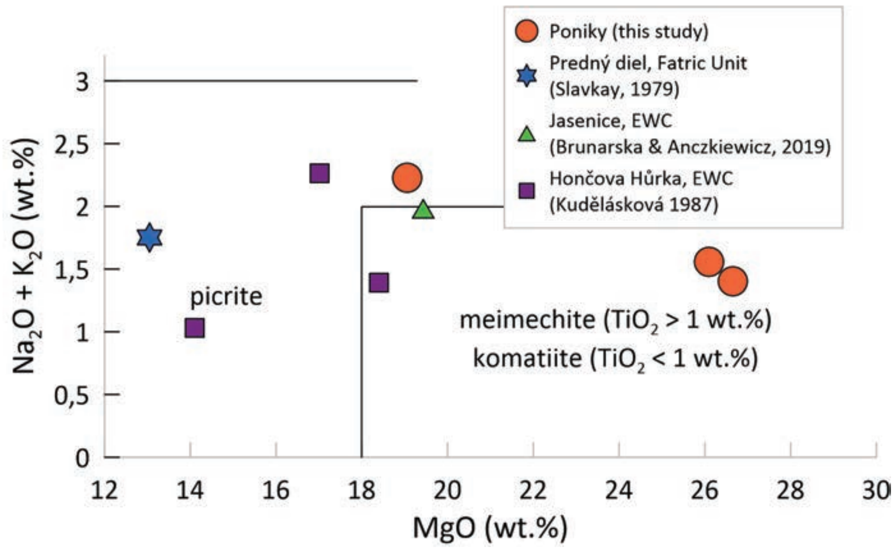

Fig. 9. IUGS classification of high MgO picritic rocks (Le Bas, 2000). A sample from Predný diel (Fatric Unit) and picritic samples from the teschenite association are shown for comparison.

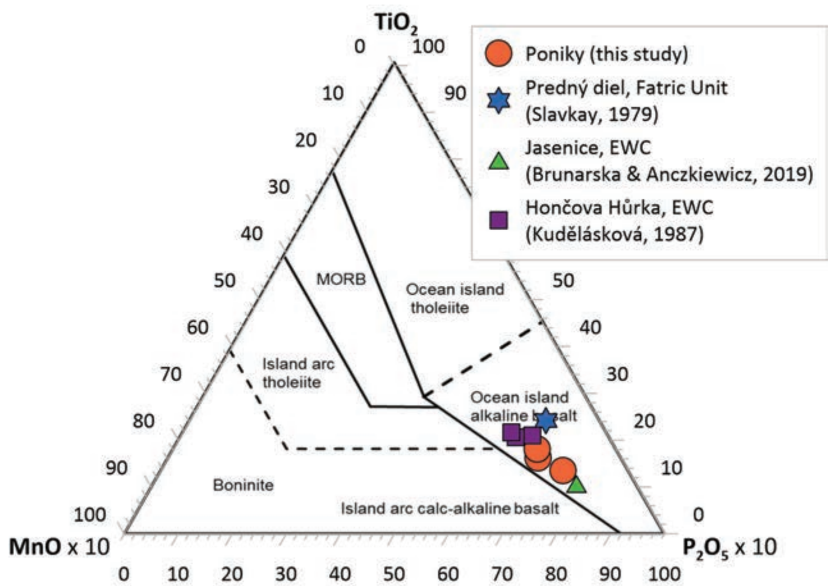

Fig. 10. Ternary discrimination diagram of TiO_2 vs MnO x 10 vs P_2O_5 x 10 (after Mullen, 1983). A sample from Predný diel (Fatric Unit) and picritic samples from the teschenite association are shown for comparison.

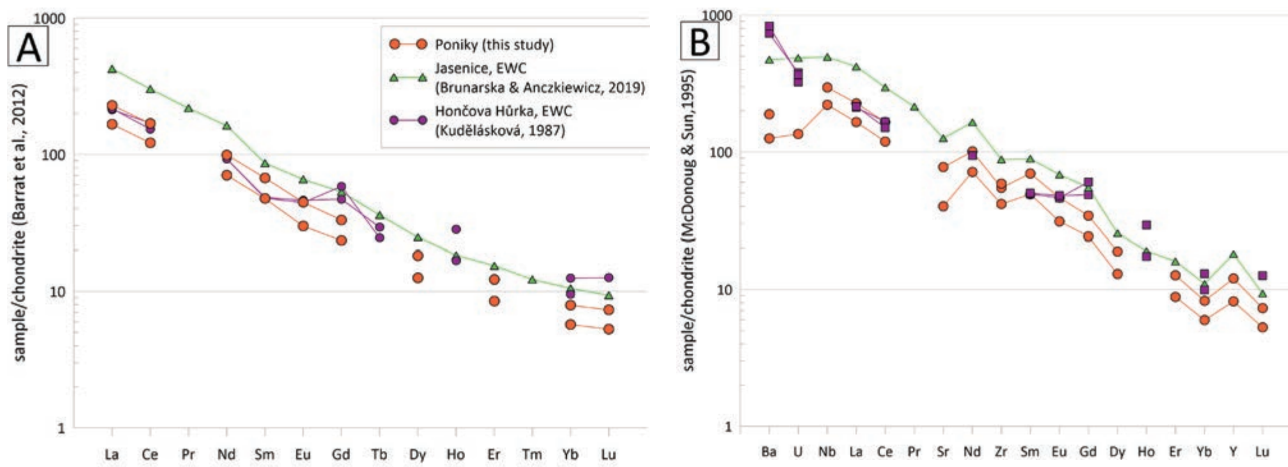

Fig. 11. A) Chondrite-normalized REE diagram (normalized to chondrite using Barrat et al., 2012); B) chondrite-normalized multielement diagram (McDonough & Sun, 1995).

Tab. 1

Selected EPM analyses of clinopyroxene. Fe^{3+} calculated by charge balance. Numbers correspond to those in Fig. 2.

Number anal.	14	15	16	17	21	23	28	51	52
Comment	Cpx II	Cpx II	Cpx II	Cpx II	Cpx II	Cpx II	Cpx I	Cpx I	Cpx I
SiO_2	47.73	49.87	49.54	48.99	47.10	46.77	49.23	48.92	48.72
TiO_2	1.21	0.92	0.66	1.09	1.46	1.74	1.34	2.28	1.86
Al_2O_3	5.97	4.28	5.43	5.01	6.29	6.85	4.70	5.52	5.49
Cr_2O_3	0.02	0.00	0.00	0.03	0.10	0.01	0.01	0.00	0.00
FeO^+	5.46	6.69	8.32	7.52	6.26	5.68	5.89	6.87	7.47
MnO	0.03	0.09	0.14	0.05	0.21	0.04	0.10	0.00	0.00
MgO	13.56	14.08	12.85	13.27	13.55	13.18	14.04	13.37	13.51
CaO	23.83	23.24	21.71	22.82	23.62	23.33	23.50	22.16	22.03
Na_2O	0.45	0.46	0.96	0.76	0.34	0.43	0.49	0.71	0.55
K_2O	0.00	0.01	0.01	0.00	0.01	0.00	0.02	0.16	0.16
TOTAL	98.27	99.63	99.61	99.54	98.92	98.02	99.32	99.99	99.79
Formula based on 6 oxygens									
Si	1.79	1.85	1.84	1.82	1.76	1.76	1.83	1.81	1.81
Ti	0.03	0.03	0.02	0.03	0.04	0.05	0.04	0.06	0.05
Al	0.26	0.19	0.24	0.22	0.28	0.30	0.21	0.24	0.24
Fe^{3+}	0.13	0.10	0.12	0.14	0.15	0.11	0.11	0.07	0.09
Fe^{2+}	0.04	0.10	0.14	0.10	0.04	0.06	0.08	0.14	0.14
Mn	0.00	0.00	0.00	0.00	0.01	0.00	0.00	0.00	0.00
Mg	0.76	0.78	0.71	0.73	0.75	0.74	0.78	0.74	0.75
Ca	0.96	0.92	0.86	0.91	0.94	0.94	0.93	0.88	0.88
Na	0.03	0.03	0.07	0.05	0.02	0.03	0.04	0.05	0.04
K	0.00	0.00	0.00	0.00	0.00	0.00	0.00	0.01	0.01
Wo	54.48	51.14	50.36	52.23	54.22	53.91	52.25	50.01	49.61
En	43.15	43.12	41.47	42.25	43.27	42.37	43.44	41.98	42.33
Fs	2.37	5.75	8.16	5.52	2.51	3.72	4.30	8.00	8.06

Tab. 2

Selected EPM analyses of amphibole. Structural formula recalculated according to Locock (2014). Numbers correspond to those shown in Figs. 2A and 2B.

Number anal.	24	25	26
SiO_2	40.58	41.00	40.49
TiO_2	4.47	4.54	4.17
Al_2O_3	12.37	11.83	12.49
FeO^+	10.62	10.99	10.66
MnO	0.16	0.22	0.26
MgO	13.78	13.74	13.64
CaO	11.61	11.75	11.63
Na_2O	3.20	3.36	3.09
K_2O	1.00	0.95	0.98
Cl	0.02	0.02	0.02
F	0.00	0.00	0.04
Total	97.80	98.41	97.46
Formula besed on 22 oxygens			
Si	6.00	6.04	6.01
Al^{IV}	2.00	1.96	1.99
Ti	0.50	0.50	0.47
Al^{VI}	0.16	0.10	0.19
Fe^{3+}	0.00	0.00	0.05
Mn^{2+}	0.00	0.03	0.01
Fe^{2+}	1.31	1.35	1.28
Mg	3.04	3.02	3.02
Mn^{2+}	0.02	0.00	0.03
Ca	1.84	1.86	1.85
Na	0.13	0.14	0.12
Na	0.79	0.82	0.77
K	0.19	0.18	0.19

Tab. 3

Selected EPM analyses of biotite. Numbers correspond to those shown in Fig. 2.

Number anal.	11	12	29	30	35
SiO	38.17	38.69	38.80	38.92	37.75
TiO_2	2.41	2.22	2.13	2.12	4.01
Al_2O_3	15.56	15.61	15.43	15.63	16.56
FeO^+	10.51	10.25	10.50	11.00	10.25
MnO	0.03	0.07	0.09	0.08	0.14
MgO	19.09	19.69	19.34	19.23	18.54
CaO	0.02	0.03	0.01	0.04	0.11
Na_2O	1.47	1.50	1.54	1.45	1.37
K_2O	8.81	8.62	8.86	8.93	8.67
Total	96.07	96.68	96.70	97.41	97.39
Formula based on 11 oxygens (all ferous iron)					
Si^{IV}	2.77	2.78	2.79	2.78	2.70
Al^{IV}	1.23	1.22	1.21	1.22	1.31
Al^{VI}	0.11	0.11	0.10	0.10	0.08
Ti	0.131	0.12	0.12	0.11	0.215
Fe^{3+}	0.00	0.00	0.00	0.00	0.00
Fe^{2+}	0.64	0.62	0.63	0.66	0.61
Mn	0.00	0.00	0.01	0.01	0.01
Mg	2.06	2.11	2.07	2.05	1.97
Ca	0.00	0.00	0.00	0.00	0.01
Na	0.21	0.21	0.22	0.20	0.19
K	0.82	0.79	0.81	0.82	0.79

Tab. 4

Selected EPM analyses of sodalite. Numbers correspond to those shown in Fig. 5.

Number anal.	18	19	20	31	32	33	34
SiO_2	36.99	37.33	36.79	37.27	36.28	36.73	36.41
TiO_2	0.00	0.00	0.00	0.00	0.00	0.00	0.00
Al_2O_3	31.52	32.20	31.98	31.87	31.31	31.38	31.46
FeO	0.15	0.19	0.05	0.40	0.13	0.08	0.07
MnO	0.00	0.04	0.00	0.00	0.00	0.00	0.06
MgO	0.02	0.05	0.00	0.01	0.00	0.00	0.00
CaO	0.06	0.06	0.07	0.10	0.01	0.02	0.01
Na_2O	24.63	24.53	24.77	24.59	25.04	24.70	24.87
K_2O	0.00	0.05	0.01	0.04	0.00	0.00	0.01
F	0.02	0.00	0.00	0.00	0.00	0.00	0.00
Cl	7.11	7.12	7.11	6.86	7.28	7.31	7.35
Total	100.50	101.57	100.78	101.14	100.05	100.23	100.24
Normalized on 12 T-cations							
Si	5.99	5.95	5.93	5.98	5.95	5.98	5.95
Al	6.01	6.05	6.07	6.02	6.05	6.02	6.05
Fe	0.02	0.03	0.01	0.05	0.02	0.01	0.01
Mn	0.00	0.01	0.00	0.00	0.00	0.00	0.01
Mg	0.01	0.01	0.00	0.00	0.00	0.00	0.00
Ca	0.01	0.01	0.01	0.02	0.00	0.00	0.00
Na	7.73	7.58	7.74	7.65	7.96	7.80	7.87
K	0.00	0.01	0.00	0.01	0.00	0.00	0.00
F	0.01	0.00	0.00	0.00	0.00	0.00	0.00
Cl	1.95	1.92	1.94	1.86	2.02	2.02	2.03

Tab. 5

Selected EPM analyses of spinel. Normalized to 3 cations and 4 oxygens; where not analytically determined, Fe^{3+} is calculated based on charge balance. Numbers correspond to those shown in Fig. 6.

Number anal.	1	2	7	8	09	010	011
SiO_2	0.01	0.02	0.01	0.00	0.09	0.00	0.00
TiO_2	0.16	0.10	0.07	0.02	0.00	0.14	0.00
Al_2O_3	52.57	52.48	53.11	50.54	52.52	50.06	52.09
Cr_2O_3	12.99	13.06	13.00	14.74	13.36	16.76	14.35
Fe_2O_3	NA	NA	NA	NA	3.37	3.25	4.10
FeO	13.00	12.76	12.86	13.31	11.20	11.51	10.80
MnO	0.12	0.14	0.11	0.14	0.00	0.00	0.00
MgO	18.11	18.41	18.44	18.06	18.99	18.74	19.37
NiO	0.32	0.29	0.25	0.26	NA	NA	NA
ZnO	0.22	0.20	0.25	0.30	NA	NA	NA
Total	97.50	97.46	98.10	97.36	99.54	100.46	100.71
Normalized on 3 cations and 4 oxygens							
Si	0.00	0.00	0.00	0.00	0.00	0.00	0.00
Ti	0.00	0.00	0.00	0.00	0.00	0.00	0.00
Al	1.68	1.67	1.68	1.63	1.65	1.58	1.62
Cr	0.28	0.28	0.28	0.32	0.28	0.35	0.30
Fe^{3+}	0.04	0.04	0.04	0.05	0.07	0.07	0.08
Fe^{2+}	0.26	0.25	0.25	0.25	0.25	0.26	0.24
Mn	0.00	0.00	0.00	0.00	0.00	0.00	0.00
Mg	0.73	0.74	0.74	0.74	0.75	0.75	0.76
Ni	0.01	0.01	0.01	0.01			
Zn	0.00	0.00	0.00	0.00			

Tab. 6

Selected EPM analyses of apatite. Numbers correspond to those shown in Fig. 5

Number anal.	36	37	38	40	41	42	43	45	46	47	48	49	50
Na_2O	0.02	0.03	0.00	0.21	0.08	0.04	0.18	0.11	0.05	0.24	0.18	0.21	0.17
MgO	0.14	0.13	0.12	0.06	0.19	0.16	0.07	0.24	0.09	0.12	0.05	0.12	0.08
CaO	53.76	54.43	54.00	49.69	54.24	54.20	50.16	53.88	53.03	47.90	48.37	49.61	50.59
SrO	0.75	0.56	0.73	5.78	0.58	0.49	4.55	0.41	1.37	6.18	6.40	5.18	4.13
MnO	0.00	0.03	0.02	0.01	0.02	0.00	0.00	0.00	0.06	0.00	0.00	0.03	0.01
FeO	0.22	0.12	0.12	0.17	0.25	0.14	0.23	0.52	0.27	0.28	0.17	0.30	0.31
Al_2O_3	0.02	0.00	0.01	0.00	0.00	0.01	0.00	0.00	0.01	0.02	0.00	0.02	0.02
Y_2O_3	0.06	0.05	0.07	0.01	0.08	0.11	0.03	0.05	0.01	0.09	0.04	0.00	0.00
La_2O_3	0.44	0.06	0.22	0.47	0.47	0.00	0.23	0.19	0.00	0.75	0.51	0.46	0.00
Ce_2O_3	0.52	0.33	0.45	0.87	0.45	0.29	0.77	0.25	0.42	0.93	0.82	0.83	0.67
Pr_2O_3	0.00	0.11	0.14	0.00	0.21	0.61	0.00	0.00	0.21	0.16	0.14	0.42	0.01
Nd_2O_3	0.20	0.15	0.10	0.13	0.34	0.29	0.00	0.16	0.03	0.18	0.00	0.18	0.00
SiO_2	0.89	0.65	0.59	0.32	0.94	0.93	0.33	1.38	0.45	0.45	0.34	0.42	0.28
P_2O_5	40.53	41.00	41.68	40.06	41.26	41.23	41.26	40.43	41.00	39.79	40.01	40.21	40.34
SO_3	0.02	0.14	0.03	0.00	0.14	0.21	0.03	0.39	0.01	0.04	0.00	0.00	0.01
F^-	1.66	1.52	1.54	1.88	1.45	1.34	1.35	1.34	1.08	1.58	1.73	1.47	1.34
Cl^-	0.32	0.27	0.28	0.07	0.30	0.30	0.17	0.36	0.35	0.18	0.12	0.15	0.13
Σ wt%	99.53	99.56	100.10	99.74	101.01	100.34	99.36	99.71	98.43	98.88	98.88	99.62	98.07
H_2O*	1.73	1.90	1.88	1.56	1.96	2.07	2.06	2.03	2.26	1.77	1.66	1.92	2.07
Σ wt%*	101.27	101.47	101.98	101.30	102.98	102.41	101.42	101.74	100.69	100.65	100.54	101.54	100.14
Empirical formula (calculated on 13 oxygens)													
Na	0.003	0.005	0.000	0.037	0.014	0.007	0.031	0.018	0.009	0.042	0.032	0.037	0.029
Mg	0.017	0.017	0.016	0.008	0.025	0.021	0.009	0.031	0.012	0.016	0.007	0.016	0.011
Ca	4.995	5.034	4.964	4.728	4.963	4.976	4.724	4.965	4.975	4.609	4.644	4.719	4.831
Sr	0.038	0.028	0.036	0.298	0.029	0.024	0.232	0.020	0.070	0.322	0.333	0.267	0.214
Mn	0.000	0.002	0.001	0.001	0.002	0.000	0.000	0.000	0.004	0.000	0.000	0.002	0.000
Fe	0.016	0.008	0.009	0.013	0.018	0.010	0.017	0.037	0.020	0.021	0.013	0.022	0.023
Al	0.002	0.000	0.001	0.000	0.000	0.001	0.000	0.000	0.001	0.002	0.000	0.002	0.002
Y	0.003	0.002	0.003	0.001	0.004	0.005	0.001	0.002	0.000	0.004	0.002	0.000	0.000
La	0.014	0.002	0.007	0.015	0.015	0.000	0.007	0.006	0.000	0.025	0.017	0.015	0.000
Ce	0.017	0.010	0.014	0.028	0.014	0.009	0.025	0.008	0.013	0.031	0.027	0.027	0.022
Pr	0.000	0.003	0.004	0.000	0.007	0.019	0.000	0.000	0.007	0.005	0.004	0.014	0.000
Nd	0.006	0.005	0.003	0.004	0.010	0.009	0.000	0.005	0.001	0.006	0.000	0.006	0.000
Si	0.077	0.056	0.051	0.028	0.080	0.079	0.029	0.118	0.040	0.040	0.031	0.037	0.025
P	2.975	2.996	3.027	3.012	2.983	2.991	3.070	2.943	3.040	3.025	3.035	3.022	3.044
S	0.001	0.009	0.002	0.000	0.009	0.013	0.002	0.025	0.001	0.003	0.000	0.000	0.001
F	0.454	0.415	0.419	0.529	0.392	0.363	0.375	0.366	0.299	0.448	0.491	0.412	0.378
Cl	0.047	0.039	0.041	0.011	0.043	0.044	0.025	0.053	0.051	0.027	0.018	0.023	0.019
OH	0.499	0.546	0.540	0.461	0.565	0.593	0.600	0.582	0.649	0.525	0.491	0.565	0.603

* H_2O content is calculated on the number of OH in empirical formula

Tab. 7

Whole-rock chemical composition of picritic rocks from the Poniky boreholes. KP-24, KP-27 (Hovorka & Slavkay, 1966), MV-81 – new analysis. For sample MV-81, only total iron as Fe_2O_3 was determined.

	KP-24	KP-27	MV-81
SiO_2	34.06	38.12	37.3
TiO_2	1.34	2.02	1.74
Al_2O_3	5.72	7.57	6.24
Fe_2O_3	6.75	6.52	9.65
FeO	3.93	4.04	
MnO	0.12	0.19	0.14
MgO	22.26	16.94	22.83
CaO	9.05	10.65	5.92
Na_2O	0.41	0.96	0.26
K_2O	0.92	1.02	0.94
P_2O_5	0.74	0.85	0.65
LOD	3.07	1.86	
LOI	10.87	8.15	13.5
Total	99.24	98.89	99.17
La	53.85		39.17
Ce	101.21		72.94
Nd	46.02		32.63
Sm	10.3		7.27
Eu	2.61		1.75
Gd	6.82		4.83
Dy	4.64		3.19
Er	2.03		1.41
Yb	1.33		0.96
Lu	0.18		0.13
Y	18.85		12.83
Ba	455		303
Co	110	117	114
Cu	48	27	39
Nb	71		53
Ni	873	1,040	1,232
Sc	18	21	15
Sr	562		291
V	173		138
Zn	135	117	124
Zr	209	224	159
B	21.4	24.5	
Cr	680	710	
Ga	14	10	
U			1
Th			8

Discussion

Petrogenesis

The chemical signature of mantle-crust interaction in subduction zones is characterized by a negative Nb-Ta anomaly (Pearce, 2008). Our sample does not display such an anomaly (Fig. 11B); we thus suggest that the studied melt is a product of intraplate magmatic activity and was not modified by subduction processes. The absence of an Eu anomaly suggests limited plagioclase fractionation and supports a relatively primitive, mantle-derived magma source. This interpretation is also supported by the high whole-rock Mg# (> 0.75). However, some degree of mantle metasomatism cannot be ruled out. First, Sr-rich rims on apatites, which were probably formed during late magmatism by residual melts enriched in Sr, volatiles, LREE, and LILE, as suggested by Zhang et al. (2011). Secondly, Ti-rich amphibole (kaersutite) is not commonly found in primary melts (Martin, 2007). The presence of these phases thus suggests that the magma that formed the picritic rocks near Poniky was derived from a metasomatized mantle source (Pilet et al., 2008; O'Reilly & Griffin, 2000).

Alkaline affinity

All presented results, including mineral composition, mineral chemistry and whole-rock chemistry, are consistent with the interpretation that the studied meimechites formed as part of an alkaline volcanic series. This interpretation is clearly supported by the newly documented occurrence of sodalite, a characteristic phase of alkaline rocks (Deer et al., 2013). Moreover, the strong enrichment in LILE, the high LREE content relative to HREE, and the elevated P_2O_5 content (> 0.65 wt%) are consistent with an alkaline affinity. The analysed samples are equivalent to oceanic-island alkaline basalts (Fig. 10). Most importantly, by comparing these data with picrite occurrences from the External Western Carpathians, we infer a genetic similarity between these rocks and the teschenite-picrite association. (Figs. 10, 11A, B) (Brunarska & Anczkiewicz, 2019; Kudělásková, 1987).

Regional comparison and tectonic implications

Hovorka & Slavkay (1966) considered the relationship between the Poniky picrites and the dolomites to be a normal stratigraphic relationship, i.e., synsedimentary volcanism. However, the relationship between the overlying and underlying complexes could not be clearly demonstrated due to the low drill core yield (Spišiak & Hovorka, 2000). Because the host dolomites were affiliated with the Hronic Unit, this was the only documented occurrence of such volcanic rocks in the Hronic Unit. However, similar alkaline volcanic rocks (although significantly altered) were documented near Banská Bystrica at Predný diel in carbonate rocks of the Fatric Unit (borehole ŠŠ II, Fig. 1; Slavkay, 1979), and, in fact, they are widespread in the Fatric Unit (Hovorka & Spišiak, 1988; Spišiak & Hovorka, 1997). This raised the question of whether similar rocks could occur in two different tectonic units with allochthonous provenance. From a lithostratigraphic perspective, based on current knowledge, there is no problem with classifying the studied Mesozoic sequence as part of the Hronicum (Fig. 1a). However, correlation with other picrite occurrences near Banská Bystrica also suggests an alternative interpretation: that the host dolomites belong to the Fatric Unit and that the studied meimechite occurrence is one of many manifestations of Cretaceous alkaline volcanic activity documented in the Fatric Unit (Spišiak & Hovorka, 2000). Taking all available evidence into account, the most plausible interpretation is that the Fatric and Hronic tectonic units were already in close proximity during the volcanic activity discussed herein.

Ivan (1991) documented an occurrence of a metamorphosed picritic rock near Medzev in the Gemeric Unit. However, this occurrence differs significantly in chemical composition from the picritic rock presented from Poniky. It has markedly lower TiO_2 (0.48 wt%), P_2O_5 (0.14 wt%), and alkali element concentrations (0.01 wt% Na_2O, 0.01 wt% K_2O), as well as lower REE concentrations, which exclude the possibility that it is a part of the same alkaline suite. In fact, it is interpreted as a differentiated basic (MOR) magma associated with basalts of the Gelnica Group (Ivan, 1991). Therefore, the picritic rock from Medzev is genetically and geochronologically unrelated to the studied rocks from Poniky.

Conclusion

- The mineral composition of picritic rocks from the Poniky area is consistent with picrites associated with alkaline rocks. This classification is supported not only by the presence of sodalite but also by whole-rock chemical composition.
- The analysed picritic rocks are equivalent to Cretaceous alkaline basalts/basanites occurring in the Fatric Unit of the Western Carpathians. Consequently, they are also similar in composition to picrites from the 'teschenite association' in the External Western Carpathians.
- Whole-rock chemical composition classifies the analysed picritic rocks as meimechites. This is the first documentation of a meimechite in the Central Western Carpathians.

Acknowledgments:

This paper is dedicated to the memory of Prof. Ján Spišiak, who passed away in April 2026. We are grateful to the chief editor, Ondrej Pelech, and the two reviewers, Irena Brunarská and Martin Ondrejka, for their insightful comments and recommendations, which significantly improved this manuscript. This work was funded by the Slovak Research and Development Agency under contract APVV-22-0092 and by the Matej Bel University Grants Agency (UGA-02-PDS-2024 and UGA-PD-05-2024).

References

Bosi, F., Biagioni, C. & Pasero, M., 2019: Nomenclature and classification of the spinel supergroup. *European Journal of Mineralogy*, 31, 1, 183–192. https://doi.org/10.1127/ejm/2019/0031-2788.

Brunarska, I. & Anczkiewicz, R., 2019: Geochronology and Sr-Nd-Hf isotope constraints on the petrogenesis of teschenites from the type-locality in the Outer Western Carpathians. *Geologica Carpathica*, 70, 3, 222–240. https://doi.org/ 10.2478/geoca-2019-0013.

Buriánek, D., Kropáč, K. & Dolníček, Z., 2013: Ultrabazické horniny těšínitové asociace v západní části Slezské jednotky. *Geologické výzkumy na Moravě a ve Slezsku*, 20, 1–2, 79–84.

Deer, W. A., Howie, R. A. & Zussman, J., 2013: An introduction to the rock-forming minerals. Mineral Society of Great Britain and Ireland. *Stevenage, Berforts Information Press*, 510 pp.

Hawthorne, F. C., Oberti, R., Harlow, G. E., Maresch, W. V., Martin, R. F., Schumacher, J. C. & Welch, M. D., 2012: Nomenclature of the amphibole supergroup. *American Mineralogist*, 97, 11–12, 2031–2048. https://doi.org/10.2138/am.2012.4276.

Hovorka, D., 1976: Predterciérne formácie bazitov Západných Karpát. *Mineralia Slovaca*, 2 8, 113–132.

Hovorka, D. & Slavkay, M., 1966: Pikrit od Poník. *Geologické práce, Správy*, 39, 41–51.

Hovorka, D. & Spišiak, J., 1988: Vulkanizmus mezozoika Západných Karpát. *Bratislava, Veda*, 272 pp.

Ivan, P., 1991: Metamorfovaný pikrit zo Strážneho vrchu pri Medzeve (gelnická skupina, paleozoikum gemerika). *Mineralia Slovaca*, 23, 155–159.

Kamenetsky, V. S., Crawford, A. J. & Meffre, S., 2001: Factors Controlling Chemistry of Magmatic Spinel: an Empirical Study of Associated Olivine, Cr-spinel and Melt Inclusions from Primitive Rocks. *Journal of Petrology*, 42, 4, 655–671. https://doi.org/10.1093/petrology/42.4.655.

Kerr, A. C. & Arndt, N. T., 2001: A Note on the IUGS Reclassification of the High-Mg and Picritic Volcanic Rocks. *Journal of Petrology*, 42, 11, 2169–2171. https://doi.org/10.1093/petrology/42.11.2169.

Kudělásková, J., 1987: Petrology and Geochemistry of Selected Rock Types of Teschenite Association, Outer Western Carpathians. *Geologický zborník – Geologica Carpathica*, 38, 5, 545–573.

Kynický, J., Xu, C., Bajer, A., Samec, P. & Kynická, A., 2009: Nové výzkumy v horninách těšínitové asociace: fluorapatit se zvýšenými obsahy Sr a REE. *Geologické výzkumy na Moravě a ve Slezsku*, 66–69.

Le Bas, M. J., 2000: IUGS Reclassification of the High-Mg and Picritic Volcanic Rocks. *Journal of Petrology,* 41, 10, 1467–1470. https://doi.org/10.1093/petrology/41.10.1467.

Locock, A. J., 2014: An Excel spreadsheet to classify chemical analyses of amphiboles following the IMA 2012 recommendations. *Computers & Geosciences*, 62, 1–11. https://doi.org/10.1016/j.cageo.2013.09.011.

Mahmood, A., 1973: Petrology of the teschenitic rock series from the type area of Cieszyn (Teschen) in the Polish Carpathians. *Annales Societatis Geologorum Poloniae*, 43, 2, 153–216.

Martin, R. F., 2007: Amphiboles in the Igneous Environment. *Reviews in Mineralogy and Geochemistry*, 67, 1, 323–358. https://doi.org/10.2138/rmg.2007.67.9.

McDonough, W. F. & Sun, S. S., 1995: The composition of the Earth. Chemical Geology, 120, 3–4, 223–253. https://doi.org/10.1016/0009-2541(94)00140-4.

Mikuš, T., Spišiak, J., Sýkora, M. & Demko, M., 2006: Chemical composition of spinels from Mesozoic alkali basalts of the Western Carpathians: implications for sources of detrital spinels in flysch sediments. *Geologica Carpathica*, 57, 6, 447–460.

Morimoto, N., 1988: Nomenclature of pyroxenes. *Bulletin de Minéralogie*, 111, 5, 535–550.

Mullen, E. D., 1983: $MnO/TiO_2/P_2O_5$: a minor element discriminant for basaltic rocks of oceanic environments and its implications for petrogenesis. *Earth and Planetary Science Letters*, 62, 1, 53–62. https://doi.org/10.1016/0012-821X(83)90070-5.

Ondrejka, M., Vojtko, R., Putiš, M., Chew, D. M., Olšavský, M., Uher, P., Nemec, O., Drakou, F., Molnárová, A. & Spišiak, J., 2022: Permian A-type rhyolites of the Drienok Nappe, Inner Western Carpathians, Slovakia: Tectonic setting from in-situ zircon U-Pb LA-ICP-MS dating. *Geologica Carpathica*, 73, 2, 123–136. https://doi.org/10.31577/GeolCarp.73.2.2.

O'Reilly, S. Y. & Griffin, W. L., 2000: Apatite in the mantle: implications for metasomatic processes and high heat production in Phanerozoic mantle. *Lithos*, 53, 3–4, 217–232. https://doi.org/10.1016/S0024-4937(00)00026-8.

Pearce, J. A., 2008: Geochemical fingerprinting of oceanic basalts with applications to ophiolite classification and the search for Archean oceanic crust. *Lithos*, 100, 1–4, 14–48. https://doi.org/10.1016/j.lithos.2007.06.016.

Pilet, S., Baker, M.B. & Stolper, E.M., 2008: Metasomatized Lithosphere and the Origin of Alkaline Lavas. *Science,* 320, 5878, 916–919. https://doi.org/10.1126/science.115656

Slavkay, M., 1971: Ložiská polymetalických rúd pri Ponikách. *Mineralia Slovaca*, 11, 3, 181–213.

Slavkay, M., 1979: Ďalšie výskyty ultrabázických efuzív v chočskom a krížňanskom príkrove pri Banskej Bystrici. *Mineralia Slovaca*, 11, 3, 239–245.

Slavkay, M., Tomko, I., Lukaj, M. & Barkáč, Z., 1968: Poniky – Pb rudy, záverečná správa z etapy vyhľadávacieho prieskumu a výpočet zásob so stavom k 30. XI. 1968. *Manuscript. Bratislava, Archive of St. Geol. Inst. of D. Štúr* (arch. no. 22903), 274 pp.

Šmíd, B., 1962: Přehled geologie a petrografie hornin těšínitové asociace na severním úpatí Beskyd. *Geologické práce, Zošit,* 63, 53–60.

Spišiak, J. & Hovorka, D., 1997: Petrology of the Western Carpathians Cretaceous Primitive Alkaline Volcanics. *Geologica Carpathica*, 48, 2, 113–121.

Spišiak, J. & Hovorka, D., 2000: Picrite Rocks in the Vicinity of Banská Bystrica (Krížna unit, Western Carpathians). *Slovak Geological Magazine*, 6, 4, 419–429.

Szopa, K., Włodyka, R. & Chew, D., 2014: LA-ICP-MS U-Pb apatite dating of Lower Cretaceous rocks from teschenite-picrite association in the Silesian Unit (southern Poland). *Geologica Carpathica*, 65, 4, 273–284. https://doi.org/10.2478/geoca-2014-0018.

Tischendorf, G., Förster, H.-J., Gottesmann, B. & Rieder, M., 2007: True and brittle micas: composition and solid-solution series. *Mineralogical Magazine*, 71, 3, 285–320. https://doi.org/10.1180/minmag.2007.071.3.285.

Zhang, W., Shao, J., Wang, R., Xu, X., Che, X. & Yang, Y., 2011: Sr-rich apatite from the Dangzishan leucitite-ijolite xenoliths (Heilongjiang Province): Mineralogy and mantle-fluid metasomatism. *Chinese Science Bulletin*, 56, 1, 53–63. https://doi.org/10.1007/s11434-010-4228-7.

Pikritické horniny (mejmečity) z Poník: mineralógia a petrológia (Západné Karpaty)

Pikrit je definovaný ako hypoabysálna, často porfýrická hornina s vysokým obsahom mafických minerálov a so zvýšeným obsahom MgO v porovnaní s bazaltmi (> 12 hm. %; Le Bas, 2000). Výskyty pikritov sú v Západných Karpatoch zriedkavé. Vo Vonkajších Západných Karpatoch sa vyskytujú ako súčasť kriedovej těšínitovo-pikritovej asociácie v sliezskej jednotke (Brunarska & Anczkiewicz, 2019; Buriánek et al., 2013; Hovorka, 1976; Hovorka & Spišiak, 1988; Kudělásková, 1987; Mahmood, 1973; Šmíd, 1962; Szopa et al., 2014). Vo Vnútorných Západných Karpatoch boli obmedzené výskyty pikritov opísané len z vrtov v mezozoických sedimentárnych sekvenciách v okolí Banskej Bystrice (Hovorka & Slavkay, 1966; Hovorka & Spišiak, 1988; Slavkay, 1979). Tieto pikritické horniny majú kriedový vek a geneticky súviseli s alkalickým vulkanizmom. Ojedinelý výskyt metamorfovaného pikritu bol zdokumentovaný aj v gelnickej skupine gemerika (Ivan, 1991).

Podstatné množstvo informácií o výskyte pikritov v okolí Banskej Bystrice bolo publikované už v monografii *Mezozoický vulkanizmus Západných Karpát* (Hovorka & Spišiak, 1988). Napriek tomu v tejto práci prezentujeme nové zaujímavé mineralogické a petrologické údaje o staršej vzorke pikritu z vrtu pri Ponikách. Okrem hlavných mafických minerálov (klinopyroxén, kaersutit, flogopit) sú opísané aj spinely, apatit bohatý na Sr (až do 6,4 hm. % SrO) a sodalit. Sodalit je vo Vnútorných Západných Karpatoch zdokumentovaný po prvýkrát a spolu s minerálnym a celohorninovým chemickým zložením hornín potvrdzuje ich alkalický charakter. Petrologické údaje vrátane REE ukazujú, že tieto horniny sú ekvivalentné kriedovým vulkanickým horninám vyskytujúcim sa vo fatriku, ako aj pikritickým horninám těšínitovo-pikritovej asociácie vo Vonkajších Západných Karpatoch. Vysoký obsah MgO (> 18 hm. %) umožňuje klasifikovať tieto horniny ako mejmečity.

Doručené / Received: 27. 3. 2026
Prijaté na publikovanie / Accepted: 15. 7. 2026